

Performance evaluation of wheat straw and wood chips as sustainable biofiltration media for multi-parameter nutrient removal from dairy wastewater

Aya Foad Kamel¹, Salwa Hadi Ahmed^{1*} 

¹ Department of Environmental Engineering, College of Engineering, University of Tikrit, 34001 Tikrit, Iraq

* Corresponding author's e-mail: dr.salwahadi@tu.edu.iq

ABSTRACT

Dairy wastewater is a nutrient-rich agro-industrial effluent characterized by elevated chemical oxygen demand (COD), suspended solids, and nitrogen and phosphorus concentrations; consequently, it requires low-cost and decentralized treatment options. This study evaluated a laboratory-scale downflow biofiltration system packed with a mixed wheat-straw and wood-chip medium for multi-parameter treatment of real dairy wastewater. Four identical columns (BTF1–BTF4) were operated using particle sizes of 0.40, 2.36, 4.75, and 9.50 mm at hydraulic retention times (HRTs) of 5, 10, and 24 h. The influent contained 23.70 mg L⁻¹ PO₄³⁻, 33.15 mg L⁻¹ NO₃⁻, 413 mg L⁻¹ COD, 1.595 mg L⁻¹ total suspended solids (TSS), and 1.463 mg L⁻¹ total dissolved solids (TDS). At 24 h, BTF1 achieved the highest phosphate and COD removal efficiencies (91.27% and 76.51%, respectively), whereas BTF2 achieved the highest nitrate and TSS removal efficiencies (80.38% and 92.66%, respectively). One-way ANOVA indicated that HRT significantly affected phosphate and COD removal ($p < .001$), whereas particle-size effects were not statistically significant at $\alpha = .05$. Multiple linear regression explained 80.2% of the variance in COD removal, with HRT identified as the dominant positive predictor. A composite performance index ranked BTF2 at 24 h as the optimal overall treatment condition. A supplementary extended-operation assessment up to 72 h indicated satisfactory solids retention and partial organic-load attenuation; however, it also showed increased effluent TDS and reduced phosphate-buffering capacity after prolonged contact. These trends support the interpretation that solute leaching from the lignocellulosic media may increase as contact time and solids deposition increase. The initial acidification followed by recovery of effluent pH toward near-neutral conditions suggests progressive system stabilization. Overall, mixed lignocellulosic biofiltration appears technically feasible for decentralized dairy wastewater management, particularly in resource-limited settings.

Keywords: biofiltration, dairy wastewater, hydraulic retention time, lignocellulosic media, nutrient removal.

INTRODUCTION

Nutrient pollution of freshwater ecosystems is among the most persistent environmental challenges of the twenty-first century. Excess nitrogen and phosphorus inputs stimulate algal proliferation and eutrophication, which can cause dissolved-oxygen depletion, hypoxia, harmful algal blooms, and consequent disruption of biodiversity and ecosystem services (Álvarez et al., 2017; de-Bashan and Bashan, 2004; Othman et al., 2018; U.S. Geological Survey, 2025). Because freshwater constitutes only approximately

2.5% of global water resources, with less than 1% readily accessible, nutrient-rich wastewater streams place additional pressure on treatment infrastructure, especially in water-scarce regions (Gleick, 1998; Tarayre et al., 2016).

Dairy processing is a major source of nutrient-contaminated agro-industrial effluent. Dairy wastewater commonly contains high biological oxygen demand (BOD), COD, suspended solids, and nitrogen and phosphorus compounds derived from milk proteins, cleaning agents, and process residues (Al-Tayawi et al., 2023; Krishnamoorthy et al., 2026; Patsialou et al., 2026; Tiron et

al., 2026). Untreated dairy effluents add further eutrophication pressure and impose a large biochemical oxygen demand on receiving waters (Ahmed et al. 2024). Therefore, phosphate and nitrate removal from dairy effluent is an important engineering priority, particularly for decentralized facilities in low-resource contexts where conventional activated sludge and membrane systems may be economically impractical (Al-Tayawi et al., 2023).

Recent literature has increasingly examined low-cost biofiltration systems that use locally available agricultural residues (Abaas and Ali, 2024; Tusiime et al., 2022). Lignocellulosic materials, including wheat straw, wood chips, rice husks, and barley straw, possess characteristics that are advantageous for passive water treatment: high internal porosity (60–85%; Addy et al., 2016), high organic carbon content (80–92%; Kim and Dale, 2004), hydrophilic fiber networks that provide sorption sites, and structural heterogeneity that supports attached biofilm communities (Buranov and Mazza, 2008; Lawther et al., 1995; Schmidt et al., 2002). Woodchip bioreactors have been applied at field scale to promote heterotrophic denitrification, whereby slowly biodegradable lignocellulosic carbon provides an electron donor for nitrate reduction (Aalto et al., 2022; Addy et al., 2016; Hoover et al., 2016; Moghaddam and Christianson, 2025; Robertson, 2010; Schipper et al., 2010). For phosphorus, removal in unmodified agricultural media may occur through particulate entrapment, electrostatic attraction, ligand exchange at hydroxyl and carboxyl groups, and co-precipitation with mineral constituents associated with the media or wastewater matrix (Deveci et al., 2024; Gong et al., 2025; Huang et al., 2020; Kumari et al., 2025; Orbuleŧ et al., 2025; Pan et al., 2023; Zhu et al., 2016). Wheat straw is particularly attractive as a filtration medium because it is renewable annually, inexpensive, hydrophilic, and rich in hemicellulose (20–30%) (Buranov and Mazza, 2008; Kim and Dale, 2004; Lawther et al., 1995). Wood chips provide a mechanically stable, slowly degradable carbon matrix that helps maintain hydraulic permeability during operation (Dittrich, 2024; Robertson, 2010; Schipper et al., 2010). Combining both materials within one filter bed enables simultaneous physical filtration, sorptive nutrient retention, and biologically mediated transformation, which is relevant to small-scale decentralized treatment applications.

Despite an expanding number of publications, so far no studies have comparatively assessed at least three particle size classes of mixed straw–woodchip media, where the reactive phase is fed with real full-strength dairy (influent) wastewater (Ahmed et al. 2023). However, most systematic comparisons of a wide range (sub-millimeter to centimeter scale) of materials with large FRG differences under effectively identical hydraulic conditions are lacking; particle size has an important controlling role over specific surface area, porosity, hydraulic conductivity and potential for biofilm development (Addy et al., 2016; Hoover et al., 2016; Moghaddam and Christianson, 2025; Schmidt et al., 2002).

This study was undertaken to fill this gap. Specific aims were: (a) validate the performance of four wheat-straw-and-woodchip biofiltration columns charged with different particle sizes (0.40–9.50 mm) at a range of HRTs; (b) compare phosphate, nitrate, COD, TSS, and TDS removal rates at HRTs of 5, 10 and 24 h; (c), determine the level of significance for key treatment parameters using one-way analysis of variance (ANOVA), pairwise post hoc comparisons and multiple linear regression; and (d) offer mechanistic explanations for observed performance trends based on established theory (Abed et al., 2022). Hypothesizing that the use of smaller-to-intermediate sizes would improve phosphate and nitrate removal through a higher contact area (and biofilm potential), it was expected for performance trends to vary between parameters, as mechanistic schemes differ from adsorptive vs. biological removal (Abed et al., 2021).

METHODS

Filtration media: selection, preparation, and characterization

Wheat straw and wood chips were obtained from local agricultural suppliers in central Iraq. These lignocellulosic materials are low-value by-products of cereal cultivation and timber processing (Buranov and Mazza, 2008; Kim and Dale, 2004), which makes them suitable for regional low-cost water-treatment applications. The media were prepared by: (a) triple washing with clean tap water to remove surface dust, clay fines, and readily soluble impurities; (b) air drying under direct solar radiation for more than 24 h until constant

mass was reached; and (c) classification into four particle-size fractions (0.40, 2.36, 4.75, and 9.50 mm) using ASTM-compliant test sieves (American Public Health Association [APHA] et al., 2023).

Wheat straw is principally composed of cellulose (30–45%), hemicellulose (20–30%), and lignin (10–20%), along with a non-core lignin component that is easily solubilized under alkaline conditions (Buranov and Mazza, 2008; Harper and Lynch, 1981; Lawther et al., 1995; Motte et al., 2014). Wood chips have a higher lignin content (22–28%) and greater mechanical stability, yielding a slower-releasing carbon matrix suitable for long-term operation (Dittrich, 2024; Robertson, 2010; Schipper et al., 2010). Table 1 summarizes literature-derived physical and chemical properties of both media types.

Experimental column configuration and setup

Four identical biofiltration columns (BTF1–BTF4) were constructed from clear Schedule-40 PVC pipe with an internal diameter of 15 cm and a total height of 50 cm. Transparent material was selected to permit visual inspection of flow distribution and media settlement. Each column was operated in downflow mode and contained three layers from bottom to top: (a) a gravel drainage layer (nominal diameter 10–20 mm; height 10 cm) to support the reactive medium and facilitate effluent drainage; (b) a 20-cm agricultural lignocellulosic layer composed of wheat straw and wood chips at the particle size assigned to the column; and (c) a sand distribution layer at the inlet to promote uniform influent spreading across the column cross-section (Abaas and Ali, 2024; Tusiime et al., 2022).

Dilute wastewater was housed in a 100-L feed reservoir mounted under constant head to ensure sustained delivery pressure (Ibrahim et al., 2024). There was a submersible pump that circulated influent from the reservoir into a manifold that split flowing to all four columns together so each column could receive an identical hydraulic loading. Physicochemical analysis: Treated effluent was collected via outlet ports into labeled sampling bottles at the base of each column. The configuration of the experiments is shown in Figure 1 and Table 2 characterizes overall specification of four columns.

Influent wastewater characterization and operating conditions

Influent wastewater was collected from a local dairy processing plant and adjusted under controlled laboratory conditions to obtain repeatable starting concentrations. The measured physicochemical characteristics of the influent are summarized in Table 3. The system was operated in continuous-flow mode, and effluent samples were collected at HRTs of 5, 10, and 24 h. All experiments were conducted under ambient laboratory conditions representative of the central Iraqi environment during the experimental period (25–32 °C; APHA et al., 2023).

Analytical methods and calibration

Physicochemical analyses were performed in accordance with Standard Methods for the Examination of Water and Wastewater (APHA et al., 2023). Phosphate was determined using a Hanna High Range Phosphate meter (Model HI717, Hanna Instruments, USA). pH and TDS were

Table 1. Physical and chemical properties of wheat straw and wood-chip filtration media (literature-derived values)

Property	Wheat straw	Wood chips	Reference
Organic matter content (%)	85–92	80–90	Zhu et al. (2016)
BET surface area (m ² g ⁻¹)	1.5–3.5	0.8–2.0	Pan et al. (2023)
Bulk density (g cm ⁻³)	0.08–0.15	0.15–0.30	Addy et al. (2016)
Porosity (%)	70–85	60–75	Addy et al. (2016)
Water absorption (g g ⁻¹)	2.9–4.0	2.9–4.0	Bouasker et al. (2014)
Cellulose content (%)	30–45	40–45	Buranov and Mazza (2008)
Lignin content (%)	10–20	22–28	Buranov and Mazza (2008)
Hemicellulose content (%)	20–30	25–40	Schmidt et al. (2002)

Note: BET – Brunauer–Emmett–Teller nitrogen adsorption method. Values represent ranges reported across multiple studies.

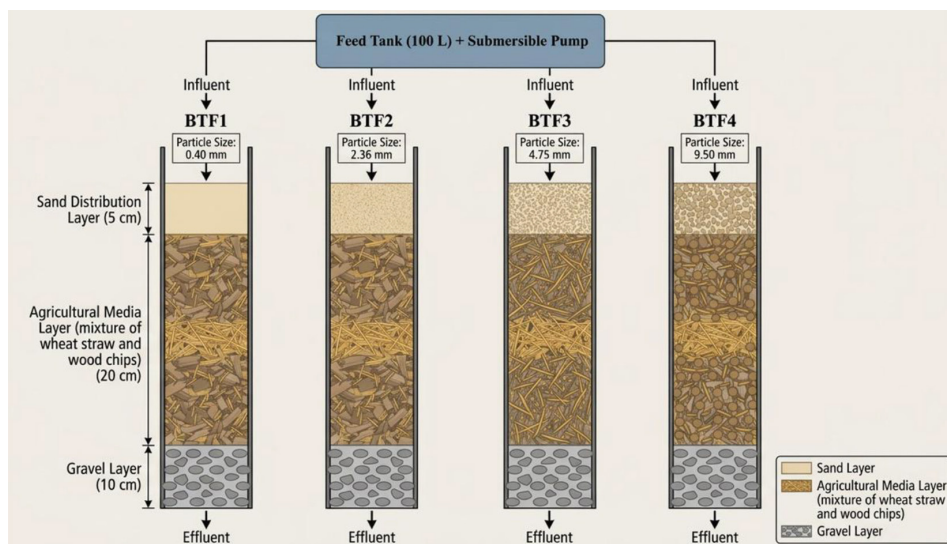


Figure 1. Schematic cross-section of the four-column downflow biofiltration system (BTF1–BTF4) showing the layered media configuration (gravel, agricultural media, sand) and flow direction

Table 2. Specifications of biofiltration columns BTF1–BTF4

Parameter	BTF1	BTF2	BTF3	BTF4
Particle size (mm)	0.40	2.36	4.75	9.50
Column diameter (cm)	15	15	15	15
Total height (cm)	50	50	50	50
Gravel layer (cm)	10	10	10	10
Media layer (cm)	20	20	20	20
Sand layer (cm)	5	5	5	5
HLR ($L\ m^{-3}\ day^{-1}$)	≈112	≈112	≈112	≈112
Flow direction	Downflow	Downflow	Downflow	Downflow
Operation mode	Continuous	Continuous	Continuous	Continuous

Note: HLR – hydraulic loading rate. All four columns operated simultaneously under identical hydraulic conditions.

Table 3. Measured physicochemical characteristics of influent dairy wastewater

Parameter	Value	Unit	Analytical method
Phosphate (PO_4^{3-})	23.70	$mg\ L^{-1}$	Hanna HI717 phosphate meter
Nitrate (NO_3^-)	33.15	$mg\ L^{-1}$	UV spectrophotometry, 220 nm
COD	413	$mg\ L^{-1}$	HACH closed-reflux colorimetric
TSS	1.595	$mg\ L^{-1}$	Gravimetric filtration (0.45 μm)
TDS	1.463	$mg\ L^{-1}$	Digital TDS/conductivity meter
pH	6.99	—	Calibrated digital pH meter
Temperature	25–32	$^{\circ}C$	Calibrated thermometer
HLR	≈112	$L\ m^{-3}\ day^{-1}$	Volumetric flow measurement

Note: All values represent the mean of triplicate measurements conducted prior to each experimental run.

measured using a calibrated OAKTON® pH/conductivity/TDS multiparameter meter (USA). COD was determined using a HACH® closed-reflux colorimetric analyzer after reactor digestion at 150 °C (HACH, Germany). Nitrate (NO_3^-) was measured spectrophotometrically using a

UV–visible spectrophotometer (UVD 3000, LABOMED, USA) at 220 nm, with baseline correction at 275 nm to account for dissolved organic matter interference. TSS was determined gravimetrically using pre-weighed 0.45- μm glass-fiber filters and a high-precision analytical balance (Adventurer Pro

AV313C, ±0.001 g, Ohaus, Switzerland). Samples were transported on ice and analyzed within 4 h of collection (Ahmed et al., 2024).

Removal efficiency (R, %) for each parameter was calculated as:

$$R(\%) = \left[\frac{(C_0 - C_e)}{C_0} \right] \times 100 \quad (1)$$

where: C_0 is the measured influent concentration and C_e is the measured effluent concentration (both in mg L^{-1}).

Statistical analysis

Because the four columns represent distinct treatment conditions (different particle sizes) rather than replicated measurements of the same condition, the primary analysis is appropriately comparative. However, each column was tested at three HRT levels (5, 10, and 24 h), generating $n = 3$ observations per column and $n = 4$ observations per HRT level. This design allows for one-way ANOVA to determine if particle size (between columns) or HRT (between time points) has a significant effect on removal efficiency of each water quality parameter (Ahmed and Abduljabbar, 2023).

The effect of particle size (column: BTF1–BTF4; $k = 4$ groups, $n = 3$ observations per group) and the effect of HRT (5, 10, and 24 h; $k = 3$ groups, $n = 4$ observations per group) were tested independently. When ANOVA indicated a statistically significant effect ($\alpha = .05$), independent-samples t-tests with Bonferroni correction were used for post hoc pairwise comparisons to control the family-wise error rate (Wasserstein et al., 2019). To predict COD removal efficiency as a function of HRT (h) and particle size (mm), a multiple linear regression model

was developed. Model adequacy was evaluated based on R^2 , adjusted R^2 and statistical significance of individual regression coefficients (Abdullah and Ahmed, 2026).

To obtain an integrated measure of overall treatment performance, a composite performance index (CPI) was calculated as the arithmetic mean of the removal efficiencies for PO_4^{3-} , NO_3^- , COD, TSS, and TDS for each column–HRT combination. Descriptive statistics, including mean, standard deviation, range, and coefficient of variation, were also calculated for all removal parameters across the twelve tested conditions to characterize central tendency and relative variability. Because of the small sample size ($n = 3$ –4 per group) and the associated low statistical power, Type II error remains possible. Therefore, the statistical outcomes should be interpreted as exploratory evidence of treatment trends rather than definitive hypothesis confirmation. In accordance with Wasserstein et al. (2019), p values were interpreted together with effect estimates and descriptive performance patterns. All statistical analyses were conducted using Python 3.11 (SciPy v1.11; NumPy v1.24).

RESULTS

Overall treatment performance at 24-hour HRT

As shown in Table 4 and illustrated in Figure 2, treatment performance was strongest and most uniform at the 24-h HRT across all columns. All measured parameters exhibited substantial reductions, indicating that the wheat-straw and wood-chip medium functioned as a multifunctional treatment substrate. However, maximizing one

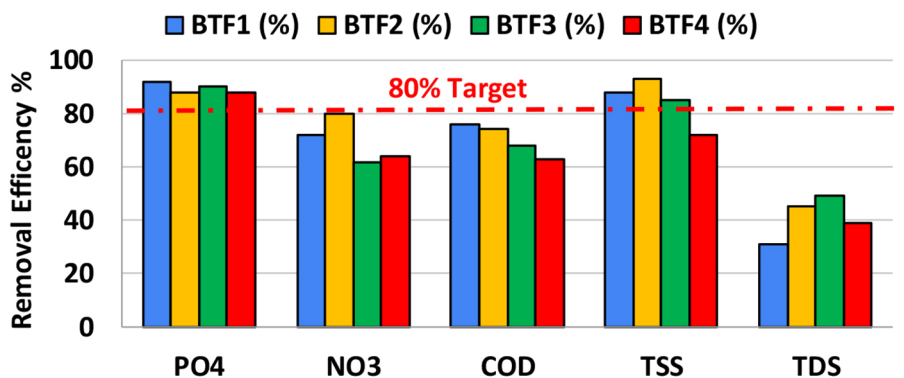


Figure 2. Multi-parameter removal efficiency (%) of biofiltration columns BTF1–BTF4 at 24-h HRT. The dashed line indicates the 80% performance threshold

Table 4. Effluent quality and removal efficiencies at 24-h HRT

Column	PO ₄ ³⁻	R%	NO ₃ ⁻	R%	COD	R%	TSS	R%	pH
Influent	23.70	—	33.15	—	413	—	1,595	—	6.99
BTF1	2.07	91.27	9.28	72.00	97	76.51	197	87.65	7.2
BTF2	2.75	88.40	6.50	80.38	104	74.82	117	92.66	6.2
BTF3	2.35	90.08	12.53	62.20	131	68.28	248	84.45	6.0
BTF4	2.75	88.40	11.83	64.31	153	62.95	449	71.85	6.3

Note: All concentrations are in mg L⁻¹ except pH. R% – removal efficiency. All values are single-run measurements.

response variable did not necessarily maximize the others, because phosphate retention, nitrate removal, COD attenuation, and TSS capture are governed by partially distinct physicochemical and biological mechanisms (Addy et al., 2016; Pan et al., 2023; Schipper et al., 2010).

Removal efficiencies across hydraulic retention times

Table 5 presents removal efficiencies across the full dataset for all HRTs and columns. Phosphate and COD removal generally increased with HRT. Nitrate removal exhibited more column-specific behavior: BTF2 increased progressively from 69.0% at 5 h to 80.4% at 24 h, whereas BTF3 showed high nitrate removal after 5 h (88.8%) followed by lower values at 10 and 24 h (80.7% and 62.2%, respectively); demonstrating that compared with phosphate or COD, nitrate performance was comparatively more sensitive to transient operating conditions (Kamel and Ahmed, 2026) (Figures 3, 4).

pH variation and system stabilization

All four columns (Table 6; Figure 5) exhibited a characteristic biphasic pH profile. During the first 5–10 h, the influent pH of 6.99 shifted toward acidic conditions (3.9–6.5), probably because of rapid hydrolysis and dissolution of hemicellulose-derived short-chain organic acids, including acetic and formic acids. By 24 h, effluent pH partially recovered toward near-neutral conditions (6.0–7.2), consistent with documented pH dynamics in lignocellulosic biofiltration systems (Motte et al., 2014; Saliling et al., 2007).

BTF1 (0.40 mm; finest medium) exhibited the most moderate initial acidification (pH = 6.5 at 5 h) and the strongest recovery toward near-neutral conditions (pH = 7.2 at 24 h). This response may reflect greater hydraulic resistance in the finer medium, which slowed the early desorption and washout of organic acids. By contrast, BTF2–BTF4 showed stronger early acidification (pH = 3.9–4.2 at 5 h), consistent with more rapid washout of acid leachates from more permeable media (Saliling et al., 2007).

Table 5. Complete removal efficiencies (%) at all hydraulic retention times for BTF1–BTF4

HRT	Column	R% PO ₄ ³⁻	R% NO ₃ ⁻	R% COD	R% TSS	R% TDS	Effluent pH	Influent pH
5 h	BTF1	62.9	54.2	41.4	72.0	2.6	6.5	6.99
	BTF2	65.0	69.0	46.7	73.4	63.4	4.0	6.99
	BTF3	65.4	88.8	33.4	72.3	63.6	4.2	6.99
	BTF4	63.3	61.5	49.1	70.5	60.1	4.2	6.99
10 h	BTF1	77.2	72.4	47.7	93.7	41.7	5.9	6.99
	BTF2	72.6	77.7	48.9	78.3	64.2	4.0	6.99
	BTF3	56.1	80.7	34.1	78.2	65.3	4.0	6.99
	BTF4	54.4	100.0	36.1	79.4	64.4	3.9	6.99
24 h	BTF1	91.3	72.0	76.5	87.7	30.8	7.2	6.99
	BTF2	88.4	80.4	74.8	92.7	44.7	6.2	6.99
	BTF3	90.1	62.2	68.3	84.5	48.5	6.0	6.99
	BTF4	88.4	64.3	63.0	71.8	38.6	6.3	6.99

Note: All effluent concentrations are single-run measurements. The 100.0% nitrate removal for BTF4 at 10 h corresponds to an effluent concentration below the analytical detection limit in that single run.

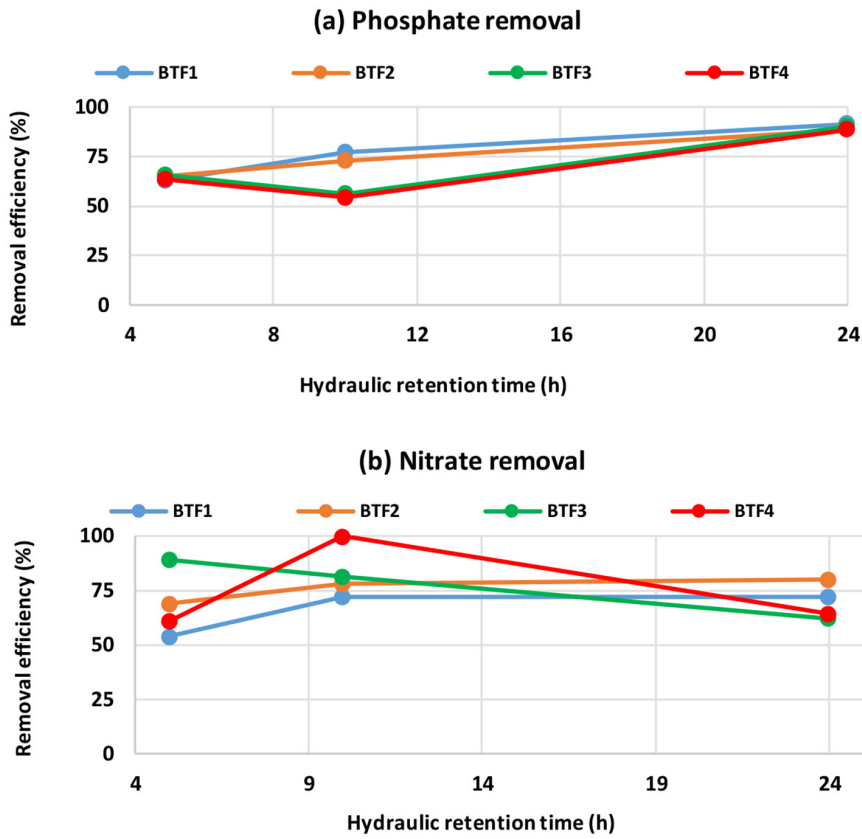


Figure 3. Effect of hydraulic retention time on (a) phosphate (PO_4^{3-}) and (b) nitrate (NO_3^-) removal efficiency for all biofiltration columns BTF1–BTF4

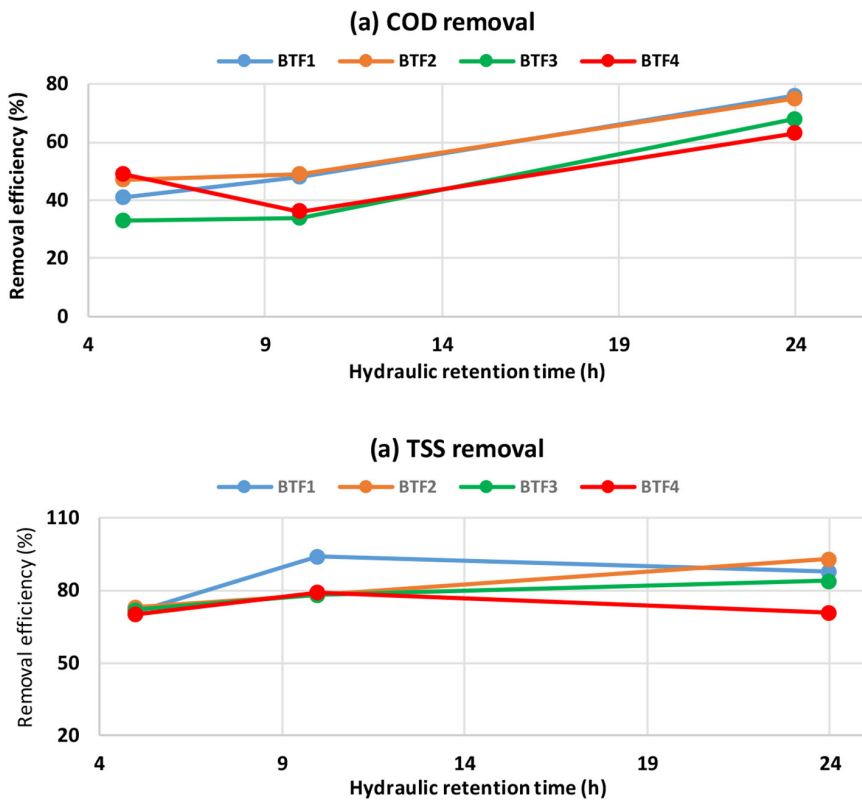


Figure 4. Effect of hydraulic retention time on (a) chemical oxygen demand (COD) and (b) total suspended solids (TSS) removal efficiency for all biofiltration columns BTF1–BTF4

Table 6. Effluent pH values across all biofiltration columns and retention times

HRT	BTF1 (0.40 mm)	BTF2 (2.36 mm)	BTF3 (4.75 mm)	BTF4 (9.50 mm)
Influent	6.99	6.99	6.99	6.99
5 h	6.5	4.0	4.2	4.2
10 h	5.9	4.0	4.0	3.9
24 h	7.2	6.2	6.0	6.3

Note: Optimal biological treatment pH range: 6.5–8.5 (Metcalf and Eddy, 2014). Recovery toward neutral pH at 24 h is consistent with depletion of readily leachable organic acid fractions.

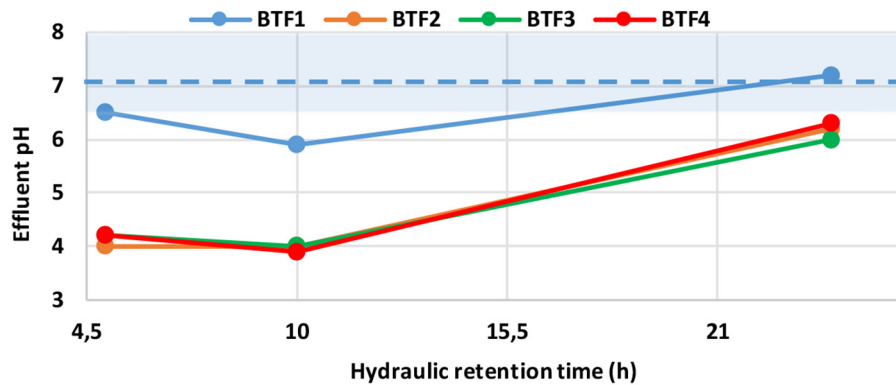


Figure 5. Effluent pH variation with hydraulic retention time across biofiltration columns BTF1–BTF4. Green shading indicates the optimal biological treatment pH range (6.5–8.5). The dashed line indicates influent pH (6.99)

Effluent phosphate concentration profile

Effluent phosphate concentration decreased with increasing HRT (Figure 6). At 24 h, effluent concentrations from all four columns converged within a narrow range of 2.07–2.75 mg L⁻¹, corresponding to 88.40–91.27% removal relative to the influent concentration of 23.70 mg L⁻¹. The pronounced concentration decrease between 10 and 24 h, particularly in BTF1, suggests that adsorption equilibrium developed progressively and was not completed within the first 10 h of contact time (Gong et al., 2025; Pan et al., 2023; Zhu et al., 2016).

Effect of particle size on removal performance

The relationship between particle size and removal efficiency at the 24-h time point is shown in Figure 7. For phosphate, a non-monotonic pattern was observed, with relatively high removal in the fine (BTF1, 0.40 mm) and intermediate (BTF3, 4.75 mm) media. This pattern is consistent with a surface-area contribution to adsorption at finer scales and a possible role of precipitation or diffusion-controlled retention under intermediate conditions (Gong et al., 2025; Pan et al., 2023). For nitrate, BTF2 (2.36 mm) showed the

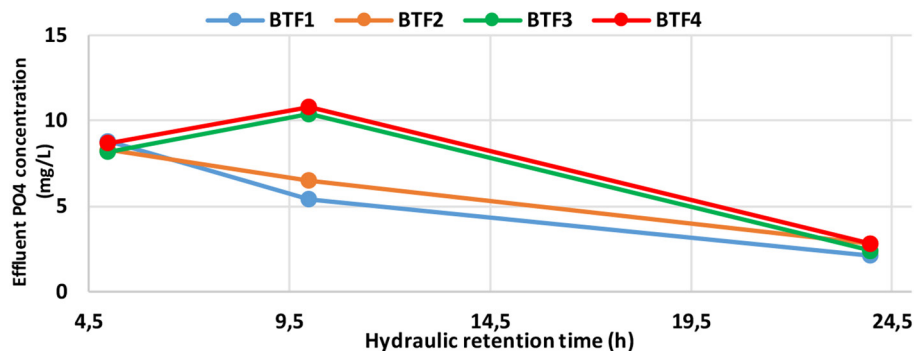


Figure 6. Effluent phosphate (PO₄³⁻) concentration as a function of hydraulic retention time for biofiltration columns BTF1–BTF4. The dashed line represents the measured influent concentration (23.70 mg L⁻¹)

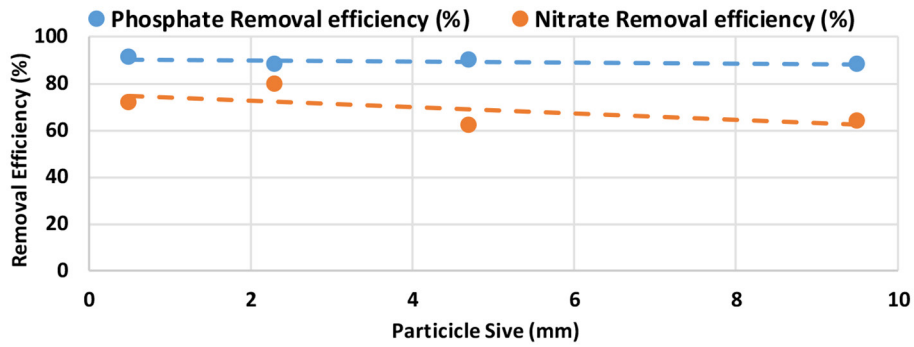


Figure 7. Scatter plot of filtration media particle size vs. removal efficiency at 24-hour HRT for phosphate and nitrate. Polynomial regression curves illustrate non-monotonic relationships reflecting contrasting mechanistic requirements for sorption vs. biological removal

highest removal, supporting the interpretation that intermediate particle size can provide a more favorable balance between hydraulic conductivity, carbon release, and anoxic biofilm microenvironments for denitrification (Moghaddam & Christianson, 2025; Schipper et al., 2010).

Overall multi-parameter performance profile

The multi-parameter performance profile at 24 h is presented in Figure 8. BTF1 and BTF3 showed strong phosphate and COD removal, whereas BTF2 exhibited the most balanced treatment profile by combining high nitrate and TSS removal with competitive phosphate reduction. BTF4 (9.50 mm), the coarsest medium, produced the weakest overall performance, suggesting that particle sizes larger than approximately 5 mm

may provide insufficient contact area and biofilm support within the tested column configuration (Addy et al., 2016; Hoover et al., 2016).

Statistical analysis of treatment performance

One-way ANOVA: Effect of particle size

For all parameters, one-way ANOVA was used to test whether particle size (BTF1–BTF4) had a statistically significant effect on removal efficiency. None of the five removal parameters showed a statistically significant particle-size effect at $\alpha = .05$. F values ranged from 0.195 (PO_4^{3-}) to 3.867 (TDS), with all p values $>.05$. The near-significant TDS result ($F = 3.867, p = .056$) should be interpreted cautiously and requires confirmation with a larger replicated dataset.

One-way ANOVA: Effect of HRT

HRT had a statistically significant effect on phosphate removal ($F = 18.264, p <.001$) and COD removal ($F = 22.181, p <.001$), as shown in Table 7. These results demonstrate that increasing contact time from 5 to 24 h significantly improved phosphate and COD treatment performance. Effects on nitrate ($F = 1.726, p = .232$), TSS ($F = 3.743, p = .066$), and TDS ($F = 0.939, p = .426$) were not statistically significant, although the TSS result approached the $\alpha = .05$ threshold.

Multiple linear regression: COD removal

A multiple linear regression model was developed to predict COD removal efficiency from HRT and particle size. The model explained a substantial proportion of variance ($R^2 = 0.802$; adjusted $R^2 = .758$). HRT was the dominant positive predictor ($\beta = 1.604, p <.001$), indicating that

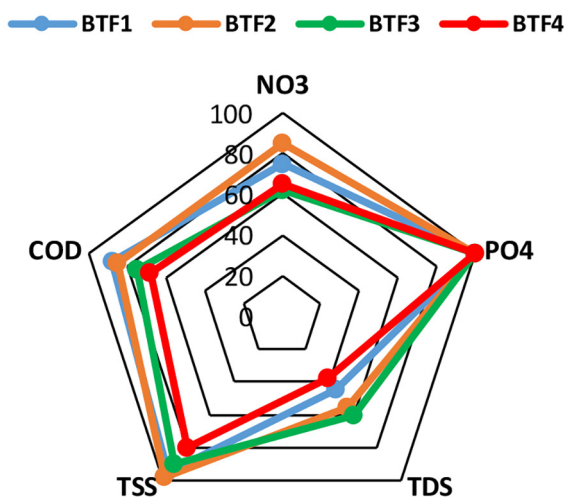


Figure 8. Radar chart providing a comprehensive visual comparison of multi-parameter removal performance (%) across biofiltration columns BTF1–BTF4 at 24-hour hydraulic retention time

Table 7. One-way ANOVA results: effects of particle size and hydraulic retention time (HRT) on removal efficiency

Parameter	F (Size)	p (Size)	Significant?	F (HRT)	p (HRT)	Significant?
R% PO ₄	0.195	.897	No	18.264	< .001	Yes
R% NO ₃	0.380	.770	No	1.726	.232	No
R% COD	0.291	.831	No	22.181	< .001	Yes
R% TSS	0.853	.503	No	3.743	.066	No
R% TDS	3.867	.056	No	0.939	.426	No

Note: Significance threshold: $\alpha = .05$. Significant? indicates statistical significance at $\alpha = .05$. Size = particle size (BTF1–BTF4, $k = 4$, $n = 3$ per group). HRT = hydraulic retention time (5, 10, 24 h; $k = 3$, $n = 4$ per group).

Table 8. Multiple linear regression results for predicting COD removal efficiency

Variable	β	SE	t	p
Intercept	22.23	6.64	3.35	.008
HRT (hours)	1.604	0.287	5.59	< .001
Particle size (mm)	-1.877	0.988	-1.90	.086

Note: $R^2 = .802$; adjusted $R^2 = .758$; $N = 12$. β = regression coefficient; SE = standard error.

each additional hour of contact time increased COD removal by approximately 1.6 percentage points on average. Particle size was a weak negative predictor ($\beta = -1.877$, $p = .086$), suggesting that larger particles may be associated with lower COD removal, although this effect was not statistically significant at $\alpha = .05$ (Table 8).

Composite performance index

CPI ranking (Table 9; Figure 10) indicated that BTF2 at 24 h was the best overall operating condition (CPI = 76.19%), followed by BTF1 at 24 h (71.64%) and BTF3 at 24 h (70.71%). This

ranking supports the interpretation that the 2.36-mm medium provided the most balanced multi-parameter treatment profile, whereas BTF1 (0.40 mm) remained preferable when maximum phosphate and COD attenuation were the principal design objectives.

Exploratory descriptive statistics

The exploratory statistical summary of the removal-efficiency dataset is provided in Table 10 and Figures 9–11. TSS showed the highest overall mean removal across all tested conditions (79.54%), followed by NO₃⁻ (73.60%) and

Table 9. Composite performance index (CPI) ranking across all column–HRT conditions

Rank	Condition	CPI (%)	Rating
1	BTF2 – 24 h	76.19	Optimal
2	BTF1 – 24 h	71.64	Good
3	BTF3 – 24 h	70.71	Good
4	BTF2 – 10 h	68.34	Moderate
5	BTF4 – 10 h	66.86	Moderate
6	BTF1 – 10 h	66.54	Moderate
7	BTF4 – 24 h	65.23	Moderate
8	BTF3 – 5 h	64.70	Moderate
9	BTF2 – 5 h	63.50	Moderate
10	BTF3 – 10 h	62.88	Moderate
11	BTF4 – 5 h	60.90	Moderate
12	BTF1 – 5 h	46.62	Low

Note: CPI = arithmetic mean of R% PO₄³⁻, R% NO₃⁻, R% COD, R% TSS, and R% TDS for each condition.

Table 10. Descriptive statistical summary of removal efficiencies across the twelve tested conditions

Parameter	Mean (%)	SD	Min	Max	Range	CV (%)
PO ₄ ³⁻	72.92	13.71	54.4	91.3	36.9	18.81
NO ₃ ⁻	73.60	12.81	54.2	100.0	45.8	17.41
COD	51.67	15.38	33.4	76.5	43.1	29.77
TSS	79.54	8.29	70.5	93.7	23.2	10.43
TDS	48.99	18.93	2.6	65.3	62.7	38.64

Note: CV = coefficient of variation; SD = standard deviation. Statistics were calculated descriptively across the 12 tested column–HRT conditions.

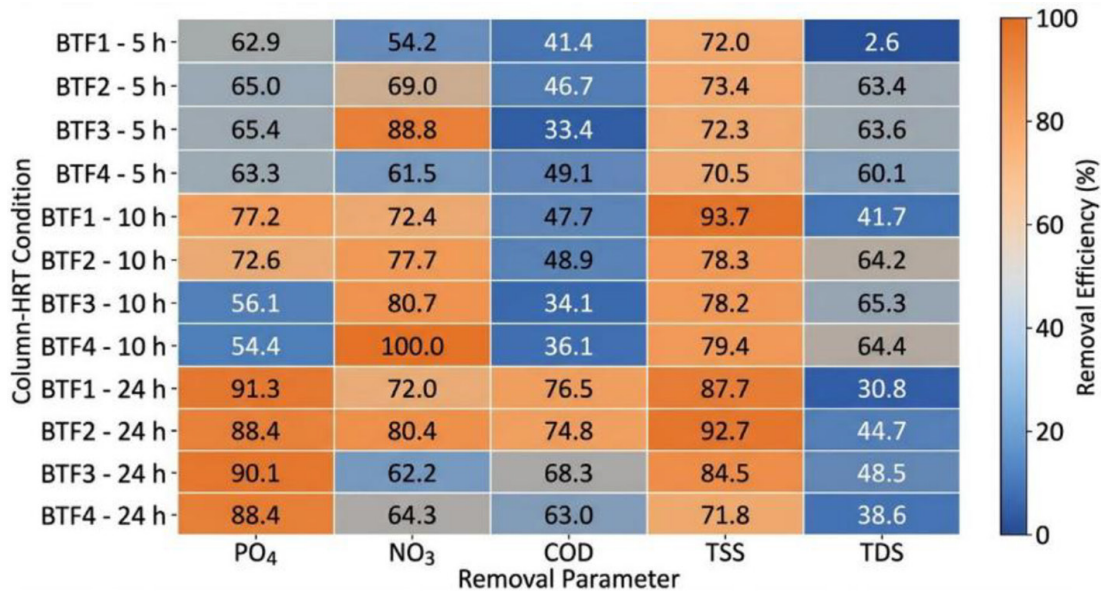


Figure 9. Heatmap of removal efficiencies (%) across all tested column–HRT conditions

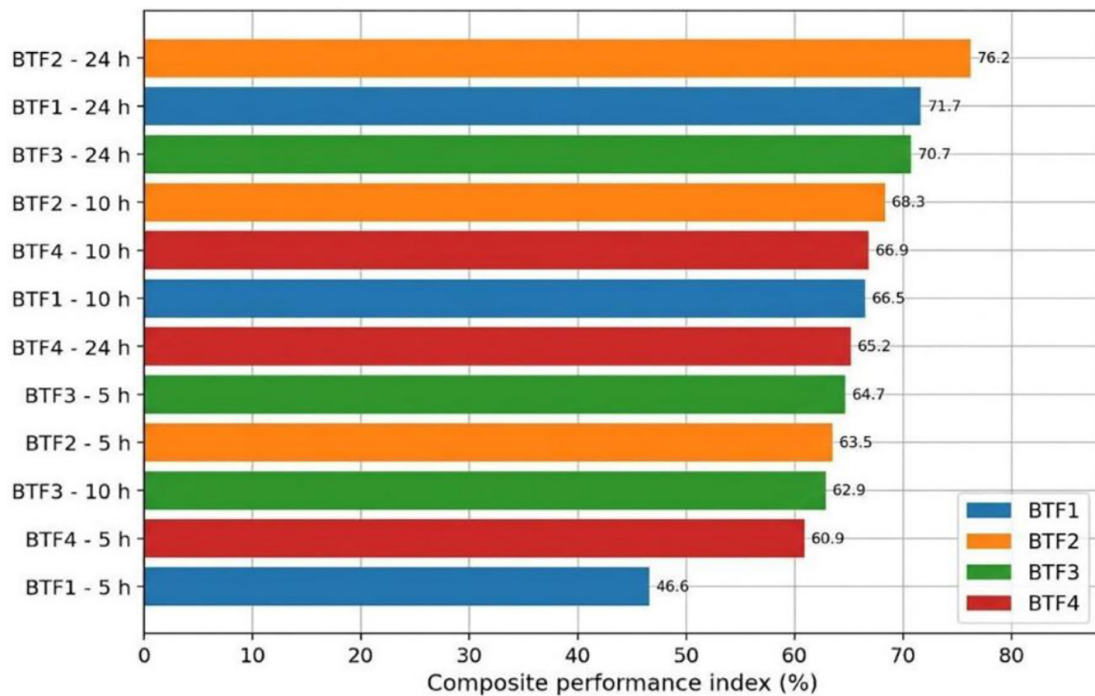


Figure 10. Composite performance index (CPI, %) for each tested column–HRT condition

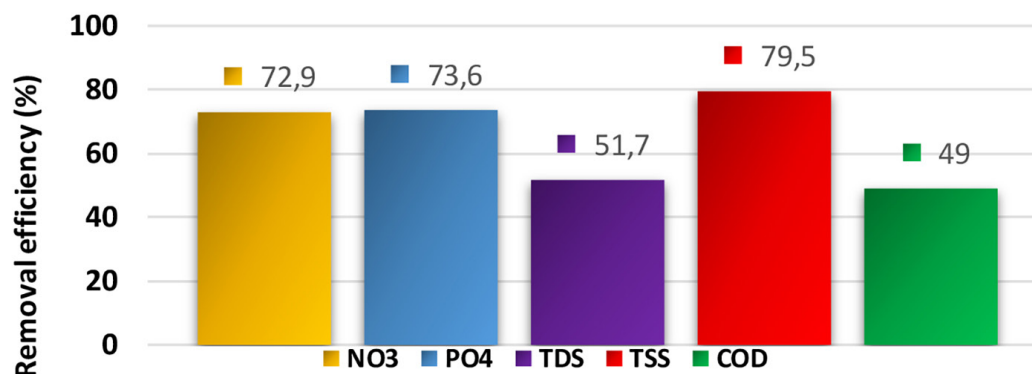


Figure 11. Descriptive mean \pm SD summary of removal efficiencies across the twelve tested conditions

PO₄³⁻ (72.93%), whereas COD and especially TDS showed lower mean removal. The coefficient of variation was lowest for TSS (10.43%), indicating relatively stable physical solids retention across the tested conditions. In contrast, TDS exhibited the highest relative variability (38.64%), consistent with the influence of media leaching and exposure time on dissolved-solids behavior.

DISCUSSION

Particle size as the primary design variable

The results indicate that particle size is an important design variable for biofiltration within the investigated range, although its effect was not statistically significant at $\alpha = .05$ in the exploratory ANOVA. This apparent discrepancy between statistical nonsignificance and observed performance differences is attributable to the small sample size ($n = 3$ per particle-size group) and variability across HRT levels. Mechanistically, particle size influences treatment through three interdependent pathways: specific surface area, hydraulic conductivity, and microbial habitat suitability (Addy et al., 2016; Hoover et al., 2016; Moghaddam and Christianson, 2025; Schmidt et al., 2002).

Fine particles provide greater external surface area per unit volume and therefore more reactive sites for phosphate adsorption through ligand exchange, electrostatic attraction, and surface complexation (Gong et al., 2025; Pan et al., 2023; Zhu et al., 2016). This likely explains the high phosphate removal observed in BTF1 (0.40 mm; 91.27%) relative to the coarser columns. For nitrate, however, the advantages of

fine particles may be offset by increased hydraulic resistance and less favorable oxygen-gradient development, which can constrain the stable anoxic microenvironments required for heterotrophic denitrification (Schipper et al., 2010). BTF2 (2.36 mm) achieved the highest nitrate removal (80.38%), outperforming both finer and coarser media, which is consistent with an intermediate-size optimum for denitrification in lignocellulosic systems (Moghaddam and Christianson, 2025; Schipper et al., 2010).

TSS removal is governed primarily by physical straining and sedimentation within the filter bed rather than by chemical or biological reactions. Although BTF1 had the smallest particle size, BTF2 produced higher TSS removal (92.66%) than BTF1 (87.65%). This result is consistent with attached-growth filtration literature indicating that intermediate media can support stable and extensive biofilm layers, thereby improving solids capture beyond mechanical straining alone (Patsialou et al., 2026; Tusiime et al., 2022).

HRT as the statistically dominant factor

ANOVA confirmed that HRT was the statistically dominant factor for phosphate ($F = 18.26$, $p < .001$) and COD removal ($F = 22.18$, $p < .001$). This finding aligns with the fundamental kinetics of both adsorption and biological degradation: phosphate adsorption via ligand exchange is a diffusion-limited process requiring progressively longer contact times to approach equilibrium (Gong et al., 2025; Pan et al., 2023), while biological COD oxidation depends on microbial–substrate interaction time that increases with HRT (Metcalf and Eddy, 2014). The regression model

reinforced this interpretation, with HRT as a highly significant positive predictor of COD removal ($\beta = 1.60$, $p < .001$, $R^2 = .80$).

Phosphate removal mechanisms

Phosphate removal in natural lignocellulosic sorbents likely involves multiple concurrent processes: (a) physical sequestration of phosphorus-containing particulates within the filter matrix; (b) adsorption through ligand exchange involving hydroxyl ($-OH$) and carboxyl ($-COOH$) functional groups in cellulose and lignin; and (c) surface complexation or precipitation with divalent cations such as Ca^{2+} and Mg^{2+} , which may be present in wheat-straw ash, wood-chip mineral fractions, and dairy wastewater (Gong et al., 2025; Huang et al., 2020; Kumari et al., 2025; Orbuleŧ et al., 2025; Pan et al., 2023; Zhu et al., 2016). Calcium phosphate precipitation under slightly alkaline conditions may also contribute to phosphate retention. The 24-h phosphate removal efficiency (88–91%) is within the range reported for several agricultural-waste biochar sorbents (Gong et al., 2025; Pan et al., 2023).

Nitrate removal and biological denitrification

Nitrate removal in woodchip-and-straw-based systems occurs primarily through heterotrophic denitrification, in which bacterial communities, including *Pseudomonas*, *Paracoccus*, and *Thauera* spp., use organic carbon released from lignocellulose decomposition as an electron donor for the sequential reduction of $NO_3^- \rightarrow NO_2^- \rightarrow NO \rightarrow N_2O \rightarrow N_2$ under anoxic conditions (Aalto et al., 2022; Hoover et al., 2016; Schipper et al., 2010). The experimental temperature range (25–32 °C) falls within the mesophilic range favorable for denitrifying microorganisms (Hoover et al., 2016; Metcalf and Eddy, 2014). The need for longer operation to maximize nitrate removal is consistent with the time required for biofilm maturation, carbon release from the lignocellulosic matrix, and oxygen depletion within the filter bed (Aalto et al., 2022; Lin et al., 2025; Saliling et al., 2007). The observed nitrate removal range (62–80%) is consistent with the performance envelope reported by Addy et al. (2016) for woodchip bioreactors treating agricultural drainage.

COD and TSS removal

The reduction in COD from 413 to 97–153 $mg\ L^{-1}$ (63–77%) indicates combined adsorption of colloidal organic matter, physical filtration of suspended organic particles, and biological oxidation by attached aerobic heterotrophs in the upper sand and reactive media layers (Metcalf and Eddy, 2014). COD removal increased from 33–49% at 5 h to 63–77% at 24 h, indicating that biological degradation, which depends on microbial–substrate contact time, contributed substantially alongside physicochemical removal processes. TSS removal remained consistently high across all columns (70–93%), confirming effective physical straining and sedimentation within the filter bed.

pH dynamics and implications

The temporary pH decrease observed during the first 5–10 h can be attributed to rapid hydrolysis of hemicellulose and the release of short-chain organic acids from fresh lignocellulosic biomass (Motte et al., 2014; Saliling et al., 2007). The subsequent recovery to pH 6.0–7.2 by 24 h likely reflects depletion of readily leachable acidic fractions and buffering by the wastewater matrix and mineral ash components of the media. These pH dynamics are relevant to nutrient removal because phosphate adsorption is generally favored under mildly acidic to near-neutral conditions, whereas denitrification can be inhibited at pH values below 6 (Hoover et al., 2016; Metcalf and Eddy, 2014). Thus, pH recovery by 24 h coincided with improved biological nitrate removal.

Statistical interpretation of global performance patterns

The exploratory statistical analysis reinforces the mechanistic interpretation of the experimental results. The low coefficient of variation for TSS (10.43%) indicates that solids removal was relatively consistent across particle sizes and HRTs, whereas the higher coefficient of variation for TDS (38.64%) suggests that dissolved-solids behavior was more sensitive to contact time and media leaching. The CPI ranking provides an additional design-oriented interpretation: BTF2 operated at 24 h was the strongest multi-parameter condition, whereas BTF1 at 24 h remained most suitable when

phosphate and COD removal were prioritized. From a practical engineering perspective, the supplementary extended-operation dataset provides a preliminary sustainability-oriented lens for interpreting the statistical results. Although these measurements were not incorporated into the core ANOVA dataset, they indicate whether treatment trends remained directionally stable under prolonged contact. At 72 h, effluent COD remained within 93–135 mg L⁻¹ relative to an influent concentration of 413 mg L⁻¹, while effluent TSS remained within 150–284 mg L⁻¹ against an influent concentration of 1.295 mg L⁻¹. These values indicate that the wheat-straw-and-wood-chip matrix retained substantial capacity for organic-load attenuation and particulate capture beyond the primary 24-h observation window. By contrast, dissolved-phase indicators were less stable: effluent TDS increased to 797–1,291 mg L⁻¹ at 72 h compared with an influent value of 463 mg L⁻¹, and phosphate concentrations increased to 3.8–16.6 mg L⁻¹, whereas the 24-h values in the supplementary dataset were lower (2.07–2.75 mg L⁻¹). These trends suggest that extended exposure can preserve filtration-driven removal of suspended and partly biodegradable

fractions while promoting soluble-constituent release and gradual exhaustion of readily available phosphate-binding sites. This interpretation is consistent with recent evidence that denitrifying bioreactors can maintain treatment capacity after initial flushing but may also release nutrients or carbon from organic media under specific hydraulic conditions (Bauwe and Lennartz, 2025; Sanchez-Bustamante Bailon et al., 2025). Therefore, the tested media mixture appears promising for decentralized treatment in terms of short-term functional stability, but long-term sustainability should be verified through continuous-run testing that directly monitors headloss, clogging behavior, dissolved organic carbon, and media-degradation kinetics.

Comparison with previous studies

Table 11 compares the present results with selected studies on agricultural-residue biofilters and denitrifying bioreactors. The observed phosphate removal efficiency (88.40–91.27% within 24 h) is competitive with many modified agricultural-waste sorbents and exceeds the performance typically expected from unmodified

Table 11. Comparison of present study results with selected previous studies on agricultural-residue-based biofiltration systems for nutrient removal

No.	Study	System / Media	Parameter	HRT	Efficiency	Key contribution
1	Schipper et al. (2010)	Woodchip bioreactors	NO ₃ ⁻	4–24 h	40–90%	Established woodchip reactors as practical technology
2	Addy et al. (2016)	Meta-analysis woodchip	NO ₃ ⁻	3–10 h	46–88%	Identified temperature and HRT as primary drivers
3	Hoover et al. (2016)	Woodchip denitrification	NO ₃ ⁻	6–20 h	35–95%	Demonstrated temperature–HRT interaction
4	Sailling et al. (2007)	Wood chips & wheat straw	NO ₃ ⁻ / pH	24–96 h	64–85%	Confirmed combined lignocellulosic media suitability
5	Tusiime et al. (2022)	Lab-scale greywater	COD, SS	5–24 h	55–92%	Feasibility of low-cost agricultural filtration
6	Abaas & Ali (2024)	Agricultural waste biofilters	Multi-param.	5–24 h	60–95%	Confirmed Iraqi agricultural residue performance
7	Pan et al. (2023)	Agricultural-waste biochar	PO ₄ ³⁻	N/A	>90%	Elucidated surface chemistry mechanisms
8	Zhu et al. (2016)	Bismuth-impregnated biochar	PO ₄ ³⁻	N/A	82–95%	Role of surface chemistry in phosphate capture
9	Gong et al. (2025)	La/Ca-doped biochar	PO ₄ ³⁻	N/A	>95%	Ligand exchange/precipitation mechanisms
10	Moghaddam and Christianson (2025)	Review: woodchip bioreactors	NO ₃ ⁻	3–48 h	40–98%	Carbon and hydraulic enhancement strategies
11	Patsialou et al. (2026)	Attached-growth biological filter	COD, nutrients	6–24 h	65–90%	Attached-growth biofiltration for dairy effluent
12	Present study (2025)	Wheat straw & wood chips	Multi-parameter	5–24 h	63–91%	Systematic particle-size comparison using real dairy wastewater

Note: WW = wastewater; HRT = hydraulic retention time; N/A = not applicable.

biofiltration media (Deveci et al., 2024; Gong et al., 2025; Kumari et al., 2025; Pan et al., 2023; Zhu et al., 2016). The nitrate removal range (62.20–80.38%) falls within the performance range reported by Addy et al. (2016) for wood-chip bioreactors treating agricultural drainage (46–88%) and is consistent with Saliling et al. (2007), who evaluated wood-chip and wheat-straw denitrification biofilters treating aquaculture wastewater at comparable HRTs.

LIMITATIONS AND FUTURE DIRECTIONS

Absence of independent replicate runs

All reported removal efficiencies are based on single experimental runs per column–HRT condition. The absence of replicate measurements precludes the calculation of true analytical error bars, confidence intervals, or measures of measurement repeatability. Future studies should incorporate a minimum of three independent replicate runs per condition to enable robust error quantification, confidence band estimation, and formal two-way ANOVA with interaction terms.

Recommended replicate-run design for future validation

To strengthen methodological rigor in future validation, each treatment condition (column–HRT combination) should be tested through at least three independent experimental runs, with triplicate analysis of PO_4^{3-} , NO_3^- , COD, TSS, TDS, and pH for each effluent sample. This design would allow calculation of mean \pm standard deviation, 95% confidence intervals, and error bars in accordance with contemporary water-quality QA/QC practice (APHA et al., 2023). It would also support factorial statistical analysis, including two-way ANOVA to test particle-size, HRT, and interaction effects, followed by Tukey HSD or Bonferroni-adjusted post hoc comparisons. Replicate-based approaches using triplicate runs, mean \pm SD reporting, and formal statistical testing have been used in recent biofilter studies to improve clarity and reproducibility of performance trends (Jiang et al., 2025; Suhartini et al., 2025). Applying this strategy to the present design would require 36 experimental trials with triplicate analytical measurements. If time or laboratory resources are limited, partial validation

could prioritize duplicate or triplicate runs for the most relevant conditions, such as BTF1–24 h, BTF2–24 h, and BTF2–10 h.

Short-term study duration

The primary performance assessment focused on HRTs up to 24 h and therefore represents an early-stage snapshot of system behavior. A supplementary extended-operation dataset was considered only for preliminary sustainability interpretation and was not included in the core inferential statistical design. Consequently, long-term stability was not comprehensively characterized. Because lignocellulosic media undergo progressive physical and biochemical degradation over weeks to months, future studies should monitor headloss development, hydraulic conductivity, clogging behavior, porosity changes, and removal performance over extended operational periods (Sang et al., 2025).

Unverified mechanistic attributions

The reduced TDS removal efficiency was interpreted as being associated with soluble organic and inorganic leaching from the lignocellulosic media, a mechanism reported in the literature (Hartfiel et al., 2023). However, dissolved organic carbon (DOC) was not measured in the effluent, and leaching kinetics were not independently characterized. Future work should include systematic DOC monitoring and spectroscopic indicators, such as UV–visible absorbance at 254 nm, to distinguish leached organic matter from residual influent-derived constituents.

CONCLUSIONS

The study demonstrates that mixed wheat-straw-and-wood-chip biofiltration can substantially remove phosphate, nitrate, COD, and TSS from dairy wastewater. Treatment performance depended primarily on HRT and secondarily on media particle size, although particle-size effects were not statistically significant at $\alpha = .05$ within the exploratory dataset. HRT had a statistically significant effect on phosphate removal ($F = 18.26$, $p < .001$) and COD removal ($F = 22.18$, $p < .001$), identifying contact time as the principal operational variable for treatment optimization. At 24 h, BTF1 (0.40 mm) produced the

highest phosphate and COD removal (91.27% and 76.51%, respectively), whereas BTF2 (2.36 mm) achieved the highest nitrate and TSS removal (80.38% and 92.66%, respectively). These divergent optima reflect the contrasting requirements of surface-area-driven adsorption and biologically mediated denitrification in lignocellulosic systems. COD removal was described effectively by a multiple linear regression model ($R^2 = .80$; adjusted $R^2 = .76$), with HRT as the dominant predictor. When PO_4^{3-} , NO_3^- , COD, TSS, and TDS removals were integrated into the CPI, BTF2 at 24 h ranked as the best overall condition (CPI = 76.19%). Exploratory descriptive statistics showed that TSS removal was the most consistent parameter across conditions, whereas TDS exhibited the highest relative variability, consistent with early-stage leaching from lignocellulosic media. Supplementary extended-operation observations indicated that the system retained COD and particulate-removal capacity beyond 24 h but became increasingly prone to dissolved-solids release and reduced phosphate retention at longer contact times.

The pH profile showed initial acidification followed by recovery toward near-neutral conditions, consistent with organic-acid release from hemicellulose followed by progressive stabilization of the media–wastewater system. Comparisons with international benchmarks indicate that the tested system is competitive with other agricultural-residue-based biofiltration technologies and comparable to selected modified biochar systems for phosphate removal. Accordingly, mixed wheat-straw-and-wood-chip biofiltration is a promising low-cost approach for decentralized dairy wastewater management. Future work should include replicated experimental runs, longer continuous operation, DOC monitoring, blank control columns, and direct assessment of hydraulic stability to strengthen evidence for scale-up and field implementation in resource-limited settings such as Iraq.

REFERENCES

1. Foad Kamel, A. and Ahmed, S. H., (Apr. 2026), Simultaneous removal of nutrients from water using advanced sustainable technologies: A comprehensive systematic review (2005–2024), *Rafidain J. Eng. Sci.*, 4(1), 713–734, <https://doi.org/10.61268/4py6ex10>
2. Aalto, S. L., Suurnäkki, S., von Ahnen, M., Tirola, M., Pedersen, P. B. (2022). Microbial communities in full-scale woodchip bioreactors treating aquaculture effluents. *Journal of Environmental Management*, 301, Article 113852. <https://doi.org/10.1016/j.jenvman.2021.113852>
3. Abaas, E. K., Ali, S. A. K. (2024). Performance of agricultural wastes as a biofilter media for low-cost greywater treatment technology. *Journal of Engineering and Sustainable Development*, 28(6), 782–792. <https://doi.org/10.31272/jeasd.28.6.11>
4. Abdullah, K. S., Ahmed, S. H. (2026). Sustainable removal of methylene blue from water using a chitosan/date-pit biochar composite: Adsorption behavior and environmental implications. *Journal of Ecological Engineering*, 27(7).
5. Abed, M. F., Zarraq, G. A., Ahmed, S. H. (2021). Hydrogeochemical assessment of groundwater quality and its suitability for irrigation and domestic purposes in rural areas, North of Baiji City-Iraq. *Iraqi Journal of Science*, 62(7), 2296–2306. <https://doi.org/10.24996/ij.s.2021.62.7.18>
6. Abed, M. F., Zarraq, G. A., Ahmed, S. H. (2022). Assessment of groundwater pollution using aqueous geo-environmental indices, Baiji Province, Salah Al-Din, Iraq. *The Iraqi Geological Journal*, 94–104. <https://doi.org/10.46717/igj.55.1B.9Ms-2022-02-25>
7. Addy, K., Gold, A. J., Christianson, L. E., David, M. B., Schipper, L. A., Ratigan, N. A. (2016). Denitrifying bioreactors for nitrate removal: A meta-analysis. *Journal of Environmental Quality*, 45(3), 873–881. <https://doi.org/10.2134/jeq2015.07.0399>
8. Ahmed, S. H., Abduljabbar, R. A. (2023). Removal of methylene blue dye from aqueous solutions using cordia myxa fruits as a low-cost adsorbent. *Tikrit Journal of Engineering Sciences*, 30(3), 90–99. <https://doi.org/10.25130/tjes.30.3.10>
9. Ahmed, S. H., Taha, A. A. A. R. (2025). Study of the use of activated carbon prepared from the eichhornia crassipes plant for removing paracetamol from aqueous solutions. *Tikrit Journal of Engineering Sciences*, 32(4), 1–15. <https://doi.org/10.25130/tjes.32.4.30>
10. Ahmed, S. H., Abed, M. F., Sharif, S. F. A., Ibrahim, A. K. (2024). Appraising the eco-health of the Tigris River water using pollution indicators and the health risk assessment model. *Water Practice & Technology*, 19(7), 2839–2849. <https://doi.org/10.2166/wpt.2024.160>
11. Ahmed, S. H., Ibrahim, A. K., Abed, M. F. (2023). Assessing the quality of the groundwater and the nitrate exposure, North Salah Al-Din Governorate, Iraq. *Tikrit Journal of Engineering Sciences*, 30(1), 25–36.
12. Ahmed, S. H., Rasheed, E. A., Rasheed, L. A., Abdulrahim, F. R. (2024). Decolorization of cationic dye from aqueous solution by Multiwalled Carbon

- Nanotubes. *Journal of Ecological Engineering*, 25(2). <https://doi.org/10.12911/22998993/176210>
13. Al-Tayawi, A. N., Sisay, E. J., Beszédes, S., Kertész, S. (2023). Wastewater treatment in the dairy industry from classical treatment to promising technologies: An overview. *Processes*, 11(7), Article 2133. <https://doi.org/10.3390/pr11072133>
 14. Álvarez, X., Valero, E., Santos, R. M. B., Varandas, S. G. P., Sanches Fernandes, L. F., Pacheco, F. A. L. (2017). Anthropogenic nutrients and eutrophication in multiple land use watersheds: Best management practices and policies for the protection of water resources. *Land Use Policy*, 69, 1–11. <https://doi.org/10.1016/j.landusepol.2017.08.028>
 15. American Public Health Association, American Water Works Association, & Water Environment Federation. (2023). Standard methods for the examination of water and wastewater (24th ed.). APHA.
 16. Ansari, S., et al. (2026). Iron-modified barley straw biochar for nitrate and phosphate removal from wastewater. *Environmental Science and Pollution Research*. <https://doi.org/10.1007/s11356-025-37358-4>
 17. Bauwe, A., Lennartz, B. (2025). Long-term performance of a denitrifying bioreactor for the treatment of nitrate-laden agricultural drainage water in northeastern Germany. *Ecological Engineering*, 218, Article 107675. <https://doi.org/10.1016/j.ecoleng.2025.107675>
 18. Bouasker, M., et al. (2014). Chemical shrinkage of cement-based materials containing lignocellulosic fibers. *Construction and Building Materials*, 64, 187–193.
 19. Buranov, A. U., Mazza, G. (2008). Lignin in straw of herbaceous crops. *Industrial Crops and Products*, 28(3), 237–259. <https://doi.org/10.1016/j.indcrop.2008.03.008>
 20. Das, A., Mishra, S. (2025). Reimagining biofiltration for sustainable industrial wastewater treatment. *Discover Sustainability*, 6, Article 826. <https://doi.org/10.1007/s43621-025-01784-8>
 21. de-Bashan, L. E., Bashan, Y. (2004). Recent advances in removing phosphorus from wastewater and its future use as fertilizer (1997–2003). *Water Research*, 38(19), 4222–4246. <https://doi.org/10.1016/j.watres.2004.07.014>
 22. Deveci, E. U., et al. (2024). Synthesis, characterization, and phosphorus adsorption of modified biochars prepared from agricultural residues. *Water Environment Research*. <https://doi.org/10.1002/wer.11077>
 23. Dittrich, T. (2024). Water absorption behavior of lignocellulosic materials and its influence on material performance. *Materials*, 17(2), Article 211. <https://doi.org/10.3390/ma17020211>
 24. Gleick, P. H. (1998). Water in crisis: Paths to sustainable water use. *Ecological Applications*, 8(3), 571–579. [https://doi.org/10.1890/1051-0761\(1998\)008\[0571:WICPTS\]2.0.CO;2](https://doi.org/10.1890/1051-0761(1998)008[0571:WICPTS]2.0.CO;2)
 25. Gong, W., Tao, C., Tian, Z., Huang, Z., Lin, H., Qi, C., Yu, Z., Guo, L. (2025). Characterization and mechanism of phosphorus adsorption from wastewater by lanthanum calcium doped sludge/wheat straw biochar. *Frontiers in Environmental Science*, 13, Article 1604542. <https://doi.org/10.3389/fenvs.2025.1604542>
 26. Harper, S. H. T., Lynch, J. M. (1981). The chemical components and decomposition of wheat straw leaves, internodes and nodes. *Journal of the Science of Food and Agriculture*, 32(11), 1057–1062. <https://doi.org/10.1002/jsfa.2740321103>
 27. Hartfiel, L. M., Hoover, N. L., Hall, S. J., Isenhardt, T. M., Gomes, C. L., Soupir, M. L. (2023). Extreme low-flow conditions in a dual-chamber denitrification bioreactor contribute to pollution swapping with low landscape-scale impact. *Science of The Total Environment*, 877, Article 162837. <https://doi.org/10.1016/j.scitotenv.2023.162837>
 28. Hoover, N. L., Bhandari, A., Soupir, M. L., Moorman, T. B. (2016). Woodchip denitrification bioreactors: Impact of temperature and hydraulic retention time on nitrate removal. *Journal of Environmental Quality*, 45(3), 803–812. <https://doi.org/10.2134/jeq2015.03.0161>
 29. Huang, Y., Lee, X., Grattieri, M., Yuan, M., Cai, R., Macazo, F. C., Minter, S. D. (2020). Modified biochar for phosphate adsorption in environmentally relevant conditions. *Chemical Engineering Journal*, 380, Article 122375. <https://doi.org/10.1016/j.cej.2019.122375>
 30. Ibrahim, A. K., Ahmed, S. H., Abduljabbar, R. A. (2024). Adsorption of Congo Red dye from aqueous solutions using an eco-friendly adsorbent derived from buckthorn fruits. *Tikrit Journal of Engineering Sciences*, 31(1), 182–192. <https://doi.org/10.25130/tjes.31.1.16>
 31. Jiang, W., et al. (2025). Enhanced nitrogen removal from aquaculture wastewater using bioretention systems with waste-derived media. *Water*, 17(18), Article 2751. <https://doi.org/10.3390/w17182751>
 32. Kim, S., Dale, B. E. (2004). Global potential bioethanol production from wasted crops and crop residues. *Biomass and Bioenergy*, 26(4), 361–375. <https://doi.org/10.1016/j.biombioe.2003.08.002>
 33. Krishnamoorthy, S., et al. (2026). Dairy wastewater treatment technologies and their applications: A state-of-the-art review. *Results in Engineering*.
 34. Kumari, S., et al. (2025). Phosphorus adsorption and recovery from waste streams using biochar: A review. *Journal of Petroleum Exploration and Production Technology*. <https://doi.org/10.1007/s13201-025-02523-0>

35. Lawther, J. M., Sun, R., Banks, W. B. (1995). Extraction, fractionation, and characterization of structural polysaccharides from wheat straw. *Journal of Agricultural and Food Chemistry*, 43(3), 667–675. <https://doi.org/10.1021/jf00051a021>
36. Lin, J. A., et al. (2025). Nitrate removal in woodchip-based bioreactors and greenhouse gas formation tradeoffs between under- and over-treatment. *Frontiers in Environmental Science*. <https://doi.org/10.3389/fenvs.2025.1543143>
37. Metcalf & Eddy. (2014). *Wastewater engineering: Treatment and resource recovery (5th ed.)*. McGraw-Hill.
38. Miito, G. J., Alege, F. P., Ndegwa, P. M. (2025). Enhancing dairy wastewater treatment: Effects of hydraulic and organic loading rates in vermifiltration systems. *Environmental Challenges*, 20, Article 101207. <https://doi.org/10.1016/j.envc.2025.101207>
39. Moghaddam, R., Christianson, L. E. (2025). Enhancing nitrate removal in denitrifying woodchip bioreactors: A comprehensive analysis of enhancement strategies and environmental trade-offs. *Journal of Water Process Engineering*, 78, Article 108806. <https://doi.org/10.1016/j.jwpe.2025.108806>
40. Motte, J.-C., Escudié, R., Beauflis, N., Steyer, J.-P., Bernet, N., Delgenès, J.-P., Dumas, C. (2014). Morphological structures of wheat straw strongly impacts its anaerobic digestion. *Industrial Crops and Products*, 52, 695–701. <https://doi.org/10.1016/j.indcrop.2013.11.038>
41. Orbuleţ, O. D., et al. (2025). Efficient and sustainable removal of phosphates from wastewater: Recent adsorbents and mechanism insights. *Environments*, 12(8), Article 288. <https://doi.org/10.3390/environments12080288>
42. Othman, A., et al. (2018). Nanoporous sorbents for the removal and recovery of phosphorus from eutrophic waters. *ACS Sustainable Chemistry & Engineering*, 6(10), 12542–12561. <https://doi.org/10.1021/acssuschemeng.8b01809>
43. Pan, W., Xie, H., Zhou, Y., Wu, Q., Zhou, J., Guo, X. (2023). Simultaneous adsorption removal of organic and inorganic phosphorus from discharged circulating cooling water on biochar derived from agricultural waste. *Journal of Cleaner Production*, 383, Article 135496. <https://doi.org/10.1016/j.jclepro.2022.135496>
44. Patsialou, S., Pla, I., Vayenas, D. V., Tekerlekopoulou, A. G. (2026). Treatment of raw mixed dairy wastewater using an attached-growth biological filter. *Environmental Earth Sciences Proceedings*, 40(1), Article 2. <https://doi.org/10.3390/eesp2026040002>
45. Robertson, W. D. (2010). Nitrate removal rates in woodchip media of varying age. *Ecological Engineering*, 36(11), 1581–1587. <https://doi.org/10.1016/j.ecoleng.2010.01.008>
46. Saliling, W. J. B., Westerman, P. W., Losordo, T. M. (2007). Wood chips and wheat straw as alternative biofilter media for denitrification reactors treating aquaculture and other wastewaters with high nitrate concentrations. *Aquacultural Engineering*, 37(3), 222–233. <https://doi.org/10.1016/j.aquaeng.2007.06.003>
47. Sanchez-Bustamante Bailon, A. P., Margenot, A., Cooke, R. A. C., Christianson, L. E. (2025). Denitrifying bioreactors and dissolved phosphorus: Net source or sink? *Journal of Environmental Quality*, 54(4), 838–850. <https://doi.org/10.1002/jeq2.20568>
48. Sang, Y., Petrovic, I., DuPlooy, L. E., Zhang, Z., Tappero, R., Ge, M., Yang, L., Reid, M. C. (2025). Biogeochemical controls on wood degradation as a source of bioavailable carbon in denitrifying bioreactors. *Environmental Science & Technology*, 59(23), 11561–11573. <https://doi.org/10.1021/acs.est.4c13325>
49. Schipper, L. A., Robertson, W. D., Gold, A. J., Jaynes, D. B., Cameron, S. C. (2010). Denitrifying bioreactors—An approach for reducing nitrate loads to receiving waters. *Ecological Engineering*, 36(11), 1532–1543. <https://doi.org/10.1016/j.ecoleng.2010.04.008>
50. Schmidt, A. S., Mallon, S., Thomsen, A. B., Hvilsted, S., Lawther, J. M. (2002). Comparison of the chemical properties of wheat straw and beech fibers following alkaline wet oxidation and laccase treatments. *Journal of Wood Chemistry and Technology*, 22(1), 39–53. <https://doi.org/10.1081/WCT-120004433>
51. Shrestha, E., et al. (2024). Adsorption of phosphate from aqueous solution using agricultural-husk composite sorbents. *Sustainability*, 16(21), Article 9259. <https://doi.org/10.3390/su16219259>
52. Suhartini, S., Vinurila, A., Rohma, N. A., Pratama, A. P. A., Sukardi, S., Hidayat, N., Sunyoto, N. M. S., Nafi'ah, R. W., Fatriasari, W., Melville, L. (2025). Efficient tofu wastewater treatment with biofiltration using OPEFB-activated carbon. *South African Journal of Chemical Engineering*, 54, 506–518. <https://doi.org/10.1016/j.sajce.2025.09.012>
53. Tang, R., et al. (2025). Biochar: From agricultural waste byproducts to novel wastewater treatment media. *Biochar*. <https://doi.org/10.1007/s42773-025-00554-z>
54. Tarayre, C., et al. (2016). New perspectives for the design of sustainable bioprocesses for phosphorus recovery from waste. *Bioresource Technology*, 206, 264–274. <https://doi.org/10.1016/j.biortech.2016.01.091>
55. Tiron, O., et al. (2026). Enhanced nutrient and organic matter removal from dairy wastewater by a

- two-stage biological process. *Frontiers in Plant Science*. <https://doi.org/10.3389/fpls.2026.1721052>
56. Tusiime, A., Solihu, H., Sekasi, J., Mutanda, H. E. (2022). Performance of lab-scale filtration system for grey water treatment and reuse. *Environmental Challenges*, 9, Article 100641. <https://doi.org/10.1016/j.envc.2022.100641>
57. U.S. Geological Survey. (2025). Where is Earth's water? Water Science School. <https://www.usgs.gov/special-topics/water-science-school>
58. Wasserstein, R. L., Schirm, A. L., Lazar, N. A. (2019). Moving to a world beyond “ $p < 0.05$.” *The American Statistician*, 73(sup1), 1–19. <https://doi.org/10.1080/00031305.2019.1583913>
59. Wojtasik, B., et al. (2026). Improving the ecological status of surface waters through waste-derived plant filters. *Sustainability*, 18(3), Article 1203. <https://doi.org/10.3390/su18031203>
60. Zheng, H., et al. (2025). Removal of ammonia nitrogen and phosphate from livestock wastewater using magnesium-modified biochar. *Bioengineered*. <https://doi.org/10.1007/s13201-025-02598-9>
61. Zhu, N., Yan, T., Qiao, J., Cao, H. (2016). Adsorption of arsenic, phosphorus and chromium by bismuth impregnated biochar: Adsorption mechanism and depleted adsorbent utilization. *Chemosphere*, 164, 32–40. <https://doi.org/10.1016/j.chemosphere.2016.08.036>